

Catalan tables and a recursion relation in noncommutative quantum field theory

Jins de Jong, Alexander Hock, Raimar Wolkenhaar

Mathematisches Institut der Westfälischen Wilhelms-Universität*
Einsteinstr. 62, D-48149 Münster, Germany

Abstract

Correlation functions in a dynamic quartic matrix model are obtained from the two-point function through a recursion relation. This paper gives the explicit solution of the recursion by mapping it bijectively to a combinatorial structure named ‘Catalan table’. As by-product of the counting of Catalan tables we prove a combinatorial identity for the Catalan numbers. Catalan tables have a neat description as diagrams of non-crossing chords and threads.

Keywords: Catalan numbers, chord diagrams, noncommutative QFT
MSC 2010: 05A19, 05C30, 81R60

1 Introduction

The quartic matrix model is defined by the following measure on the space of self-adjoint $\mathcal{N} \times \mathcal{N}$ -matrices:

$$d\mu(\Phi) = \frac{1}{Z} \exp\left(-\mathcal{N} \operatorname{Tr}\left(E\Phi^2 + \frac{\lambda}{4}\Phi^4\right)\right) d\Phi, \quad (1)$$

where E is a positive $\mathcal{N} \times \mathcal{N}$ -matrix, λ a scalar and $d\Phi$ the standard Lebesgue measure. It was proved in [1] that the N^{th} moment of the measure is in the large- \mathcal{N} limit dominated by contributions $G_{b_0 \dots b_{N-1}}^{(N)}$ (called N -point functions) which satisfy the following recursion in terms of functions of lower order:

$$G_{b_0 \dots b_{N-1}}^{(N)} = -\lambda \sum_{l=1}^{\frac{N-2}{2}} \frac{G_{b_0 \dots b_{2l-1}}^{(2l)} \cdot G_{b_{2l} \dots b_{N-1}}^{(N-2l)} - G_{b_1 \dots b_{2l}}^{(2l)} \cdot G_{b_0 b_{2l+1} \dots b_{N-1}}^{(N-2l)}}{(E_{b_0} - E_{b_{2l}})(E_{b_1} - E_{b_{N-1}})}, \quad (2)$$

*jinsdejong@uni-muenster.de, a.hock03@uni-muenster.de, raimar@math.uni-muenster.de

with N even. The b_j are matrix indices which label the moments, and $\{E_{b_j}\}$ are the eigenvalues of the positive matrix E in (1). For the purpose of this article it is safe to set $\lambda = -1$ and to ignore it in the remainder. When not mentioned explicitly, $G^{(N)} = G_{b_0 \dots b_{N-1}}^{(N)}$.

The decomposition of the $(N = 2k + 2)$ -point function $G_{b_0 b_1 \dots b_{2k+1}}^{(2k+2)}$ according to (2) yields $2^k c_k$ terms of the form

$$\frac{\pm G_{b_p b_q}^{(2)} \dots G_{b_r b_s}^{(2)}}{(E_{b_t} - E_{b_u}) \dots (E_{b_v} - E_{b_w})} \quad (3)$$

with $p < q$, $r < s$, $t < u$, and $v < w$. However, some of them cancel. In this paper we answer the so far open questions: *Which terms survive the cancellations? Can they be explicitly characterised, without going into the recursion?* The answer will be encoded in *Catalan tables*, which are Catalan tuples of Catalan tuples. A Catalan tuple is one of > 200 mathematical structures counted by the Catalan numbers c_k . See e.g. the online Catalan addendum [2] to [3]. The Catalan tables could also be relevant for other combinatorial problems.

The same recursive equation (2) appears in the planar sector of the 2-matrix model for mixed correlation functions [4]. The distinction between even b_{2i} and odd b_{2i+1} matrix indices in (2) corresponds to the different matrices of the 2-matrix model.

The paper is organised as follows. In Sec. 2 the symmetries of $G^{(N)}$ are discussed. Afterwards, in Secs. 3 and 4 we introduce Catalan tuples, Catalan tables, certain trees and operations on them. Sec. 5 is the main part of this paper. We prove in Theorem 5.1 that the Catalan tables precisely encode the terms in the non-crossing expansion of $G^{(N)}$ with specified designated node. The Catalan numbers $c_k = \frac{1}{k+1} \binom{2k}{k}$ will count various parts of our results and will be related directly to the numbers $d_k = \frac{1}{k+1} \binom{3k+1}{k}$, which count the number of Catalan tables, see Theorem 5.3.

Both the Catalan tables and the $G^{(N)}$ can be depicted conveniently as chord diagrams with threads, which will be introduced in Appendix A. Through these diagrams it will become clear that the recursion relation (2) is related to well-known combinatorial problems [5, 6].

2 Symmetries

The two-point function is symmetric, $G_{b_p b_q}^{(2)} = G_{b_q b_p}^{(2)}$. Because there is an even number of antisymmetric factors in the denominator of each term, it follows immediately that

$$G_{b_0 b_1 \dots b_{N-1}}^{(N)} = G_{b_{N-1} \dots b_1 b_0}^{(N)}. \quad (4)$$

Our aim is to prove cyclic invariance $G_{b_0 b_1 \dots b_{N-1}}^{(N)} = G_{b_1 \dots b_{N-1} b_0}^{(N)}$. We proceed by induction. Assuming that all n -point functions with $n \leq N - 2$ are cyclically invariant, it is not difficult to check that

$$\begin{aligned}
G_{b_0 b_1 \dots b_{N-1}}^{(N)} &= \sum_{l=1}^{\frac{N-2}{2}} \frac{G_{b_0 \dots b_{2l-1}}^{(2l)} \cdot G_{b_{2l} \dots b_{N-1}}^{(N-2l)} - G_{b_1 \dots b_{2l}}^{(2l)} \cdot G_{b_0 b_{2l+1} \dots b_{N-1}}^{(N-2l)}}{(E_{b_0} - E_{b_{2l}})(E_{b_1} - E_{b_{N-1}})} \\
&= - \sum_{l=1}^{\frac{N-2}{2}} \frac{G_{b_0 b_{N-1} \dots b_{2l+1}}^{(N-2l)} \cdot G_{b_{2l} \dots b_1}^{(2l)} - G_{b_{N-1} \dots b_{2l}}^{(N-2l)} \cdot G_{b_{2l-1} \dots b_1 b_0}^{(2l)}}{(E_{b_0} - E_{b_{2l}})(E_{b_1} - E_{b_{N-1}})} \\
&= \sum_{k=1}^{\frac{N-2}{2}} \frac{G_{b_0 b_{N-1} \dots b_{N-2k+1}}^{(2k)} \cdot G_{b_{N-2k} \dots b_1}^{(N-2k)} - G_{b_{N-1} \dots b_{N-2k}}^{(2k)} \cdot G_{b_0 b_{N-2k-1} \dots b_1}^{(N-2k)}}{(E_{b_0} - E_{b_{N-2k}})(E_{b_{N-1}} - E_{b_1})} \\
&= G_{b_0 b_{N-1} \dots b_1}^{(N)} = G_{b_1 \dots b_{N-1} b_0}^{(N)}. \tag{5}
\end{aligned}$$

The transformation $2l = N - 2k$ and the symmetry (4) are applied here to rewrite the sum. This shows cyclic invariance.

Although the N -point functions are invariant under a cyclic permutation of its indices, the preferred expansion into surviving terms (3) will depend on the choice of a designated node b_0 , the root. Our preferred expansion will have a clear combinatorial significance, but it cannot be unique because of

$$\frac{1}{E_{b_p} - E_{b_q}} \cdot \frac{1}{E_{b_q} - E_{b_r}} + \frac{1}{E_{b_r} - E_{b_p}} \cdot \frac{1}{E_{b_p} - E_{b_q}} + \frac{1}{E_{b_q} - E_{b_r}} \cdot \frac{1}{E_{b_r} - E_{b_p}} = 0. \tag{6}$$

These identities must be employed several times to establish cyclic invariance of our preferred expansion.

3 Catalan tuples

Definition 3.1 (Catalan tuple). A Catalan tuple $\tilde{e} = (e_0, \dots, e_k)$ of length $k \in \mathbb{N}_0$ is a tuple of integers $e_j \geq 0$ for $j = 0, \dots, k$, such that

$$\sum_{j=0}^k e_j = k \quad \text{and} \quad \sum_{j=0}^l e_j > l \quad \text{for } l = 0, \dots, k-1.$$

The set of Catalan tuples of length $|\tilde{e}| := k$ is denoted by \mathcal{C}_k .

For $\tilde{e} = (e_0, \dots, e_k)$ it follows automatically that $e_k = 0$ and $e_0 > 0$, if $k > 0$.

Example 3.2. We have $\mathcal{C}_0 = \{(0)\}$, $\mathcal{C}_1 = \{(1, 0)\}$ and $\mathcal{C}_2 = \{(2, 0, 0), (1, 1, 0)\}$. All Catalan tuples of length 3 are given in the first column of Table 1.

Composition of Catalan tuples is possible. In fact, many of them can be defined. For our purpose, two compositions are relevant.

Definition 3.3 (\circ -composition). The composition $\circ : \mathcal{C}_k \times \mathcal{C}_l \rightarrow \mathcal{C}_{k+l+1}$ is given by

$$(e_0, \dots, e_k) \circ (f_0, \dots, f_m) := (e_0 + 1, e_1, \dots, e_{k-1}, e_k, f_0, f_1, \dots, f_m) .$$

No information is lost in this composition, i.e. it is possible to uniquely retrieve both terms. In particular, \circ cannot be associative or commutative. Consider for a Catalan tuple $\tilde{e} = (e_0, \dots, e_k)$ partial sums $p_l : \mathcal{C}_k \rightarrow \{0, \dots, k\}$ and maps $\sigma_a : \mathcal{C}_k \rightarrow \{0, \dots, k\}$ defined by

$$p_l(\tilde{e}) := -l + \sum_{j=0}^l e_j , \quad \text{for } l = 0, \dots, k-1 , \quad (7)$$

$$\sigma_a(\tilde{e}) := \min\{l \mid p_l(\tilde{e}) = a\} .$$

Then

$$\tilde{e} = (e_0, \dots, e_k) = (e_0 - 1, e_1, \dots, e_{\sigma_1(\tilde{e})}) \circ (e_{\sigma_1(\tilde{e})+1}, \dots, e_k) . \quad (8)$$

Because $\sigma_1(\tilde{e})$ exists for any $\tilde{e} \in \mathcal{C}_k$ with $k \geq 1$, every Catalan tuple has unique \circ -factors. Only these two Catalan tuples, composed by \circ , yield (e_0, \dots, e_k) . This implies that the number c_k of Catalan tuples in \mathcal{C}_k satisfies Segner's recurrence relation

$$c_k = \sum_{m=0}^{k-1} c_m c_{k-1-m}$$

together with $c_0 = 1$, which is solved by the Catalan numbers $c_k = \frac{1}{k+1} \binom{2k}{k}$.

Example 3.4. We have $(1, 0) = (0) \circ (0)$, $(2, 0, 0) = (1, 0) \circ (0)$, $(1, 1, 0) = (0) \circ (1, 0)$ and $(3, 1, 0, 0, 2, 0, 0) = (2, 1, 0, 0) \circ (2, 0, 0)$.

The other composition of Catalan tuples is a variant of the \circ -product.

Definition 3.5 (\bullet -composition). The composition $\bullet : \mathcal{C}_k \times \mathcal{C}_l \rightarrow \mathcal{C}_{k+l+1}$ is given by

$$(e_0, \dots, e_k) \bullet (f_0, \dots, f_l) = (e_0 + 1, f_0, \dots, f_l, e_1, \dots, e_k) .$$

As in the case of the composition \circ , Definition 3.3, no information is lost in the product \bullet . It is reverted by

$$\tilde{e} = (e_0, \dots, e_k) = (e_0 - 1, e_{1+\sigma_{e_0-1}(\tilde{e})}, \dots, e_k) \bullet (e_1, \dots, e_{\sigma_{e_0-1}(\tilde{e})}) . \quad (9)$$

Because $\sigma_{e_0-1}(\tilde{e})$ exists for any $\tilde{e} \in \mathcal{C}_k$ with $k \geq 1$ (also for $e_0 = 1$ where $\sigma_{e_0-1}(\tilde{e}) = k$), every Catalan tuple has a unique pair of \bullet -factors.

Example 3.6. We have $(1, 0) = (0) \bullet (0)$, $(2, 0, 0) = (1, 0) \bullet (0)$, $(1, 1, 0) = (0) \bullet (1, 0)$ and $(3, 1, 0, 0, 2, 0, 0) = (2, 0, 2, 0, 0) \bullet (1, 0)$.

Out of these Catalan tuples we will construct three sorts of trees: *pocket tree*, *direct tree*, *opposite tree*. They are all rooted planar trees. Pocket tree and direct tree are the same, but their rôle will be different. Their drawing algorithms are given by the next definitions.

Definition 3.7 (direct tree, pocket tree). For a Catalan tuple $(e_0, \dots, e_k) \in \mathcal{C}_k$, draw $k + 1$ vertices on a line. Starting at the root $l = 0$:

- connect this vertex to the last vertex ($m < l$) with an open half-edge;
- if $e_l > 0$: e_l half-edges must be attached to vertex l ;
- move to the next vertex.

For direct trees, vertices will be called *nodes* and edges will be called *threads*; they are oriented from left to right. For pocket trees, vertices are called *pockets*.

Definition 3.8 (opposite tree). For a Catalan tuple $(e_0, \dots, e_k) \in \mathcal{C}_k$, draw $k + 1$ vertices on a line. Starting at the root $l = 0$:

- if $e_l > 0$: e_l half-edges must be attached to vertex l ;
- if $e_l = 0$:
 - connect this vertex to the last vertex ($m < l$) with an open half-edge;
 - if this vertex is now not connected to the last vertex ($n \leq m < l$) with an open half edge, repeat this until it is;
- move to the next vertex.

For opposite trees, vertices will be called *nodes* and edges will be called *threads*; they are oriented from left to right.

Examples of these trees can be seen in Figure 1 and Table 1. It will be explained in Sec. 5 how these trees relate to the recursion relation (2). Especially the pocket trees will often be depicted with a top-down orientation, instead of a left-right one.

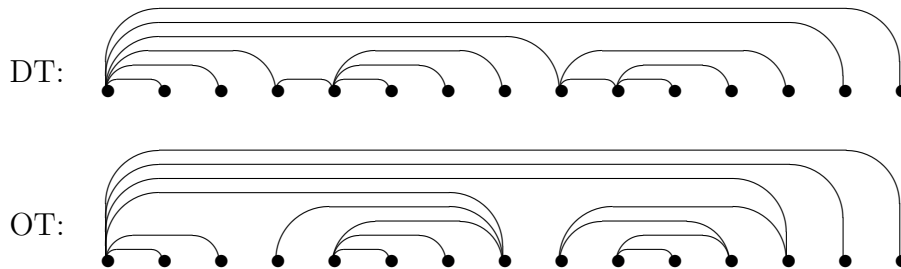


Figure 1: Direct tree (upper) and the opposite tree (lower) for the Catalan tuple $(6, 0, 0, 1, 3, 0, 0, 0, 2, 2, 0, 0, 0, 0, 0) = (5, 0, 0, 1, 3, 0, 0, 0, 2, 2, 0, 0, 0, 0, 0) \circ (0) = (5, 0, 1, 3, 0, 0, 0, 2, 2, 0, 0, 0, 0, 0) \bullet (0)$.




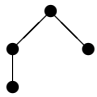


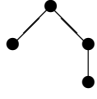


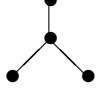





Catalan tuple	pocket tree	direct tree	opposite tree
(3,0,0,0)			
(2,1,0,0)			
(2,0,1,0)			
(1,2,0,0)			
(1,1,1,0)			

Table 1: The Catalan tuples and the corresponding trees for $k = 3$.

4 Catalan tables

A Catalan table is a ‘Catalan tuple of Catalan tuples’:

Definition 4.1 (Catalan table). A *Catalan table of length k* is a tuple $T_k = \langle \tilde{e}^{(0)}, \tilde{e}^{(1)}, \dots, \tilde{e}^{(k)} \rangle$ of Catalan tuples $\tilde{e}^{(j)}$, such that $(1 + |\tilde{e}^{(0)}|, |\tilde{e}^{(1)}|, \dots, |\tilde{e}^{(k)}|)$, the *length* tuple of T_k , is itself a Catalan tuple of length k . We let \mathcal{T}_k be the set of all Catalan tables of length k . The constituent $\tilde{e}^{(j)}$ in a Catalan table is called the j -th pocket.

Of particular relevance will be the pocket tree of the Catalan tuple $(1 + |\tilde{e}^{(0)}|, |\tilde{e}^{(1)}|, \dots, |\tilde{e}^{(k)}|)$ associated with the Catalan table $T_k = \langle \tilde{e}^{(0)}, \tilde{e}^{(1)}, \dots, \tilde{e}^{(k)} \rangle$. We will show in Sec. 5 that a Catalan table contains all information about individual terms in the expansion (3) of the N -point function $G^{(N)}$.

Example 4.2. We have

$$\begin{aligned}
\mathcal{T}_1 &= \{ \langle (0), (0) \rangle \} , \\
\mathcal{T}_2 &= \{ \langle (1, 0), (0), (0) \rangle, \langle (0), (1, 0), (0) \rangle \} \\
\mathcal{T}_3 &= \{ \langle (2, 0, 0), (0), (0), (0) \rangle, \langle (1, 1, 0), (0), (0), (0) \rangle, \langle (1, 0), (1, 0), (0), (0) \rangle, \\
&\quad \langle (1, 0), (0), (1, 0), (0) \rangle, \langle (0), (2, 0, 0), (0), (0) \rangle, \langle (0), (1, 1, 0), (0), (0) \rangle, \\
&\quad \langle (0), (1, 0), (1, 0), (0) \rangle \} .
\end{aligned}$$

Later in Fig. 2 and 3 we give a diagrammatic representation of the Catalan tables in \mathcal{T}_2 and \mathcal{T}_3 , respectively.

Recall the composition \circ from Definition 3.3 and the fact that any Catalan tuple of length ≥ 1 has a unique pair of \circ -factors. We extend \circ as follows to Catalan tables:

Definition 4.3 (\diamond -operation). The operation $\diamond : \mathcal{T}_k \times \mathcal{T}_l \rightarrow \mathcal{T}_{k+l}$ is given by

$$\langle \tilde{e}^{(0)}, \dots, \tilde{e}^{(k)} \rangle \diamond \langle \tilde{f}^{(0)}, \dots, \tilde{f}^{(l)} \rangle := \langle \tilde{e}^{(0)} \circ \tilde{f}^{(0)}, \tilde{e}^{(1)}, \dots, \tilde{e}^{(k)}, \tilde{f}^{(1)}, \dots, \tilde{f}^{(l)} \rangle .$$

Now suppose the Catalan table on the right-hand side is given. If the 0th pocket has length ≥ 1 , then it uniquely factors into $\tilde{e}^{(0)} \circ \tilde{f}^{(0)}$. Consider

$$\hat{k} = \sigma_{1+|\tilde{f}^{(0)}|} \left((1 + |\tilde{e}^{(0)} \circ \tilde{f}^{(0)}|, |\tilde{e}^{(1)}|, \dots, |\tilde{e}^{(k)}|, |\tilde{f}^{(1)}|, \dots, |\tilde{f}^{(l)}|) \right) . \quad (10)$$

By construction, $\tilde{k} = k$ so that \diamond can be uniquely reverted. Note also that Catalan tables $\langle (0), \tilde{e}_1, \dots, \tilde{e}_k \rangle$ do not have a \diamond -decomposition.

Example 4.4. We have $\langle (2, 0, 0), (0), (0), (0) \rangle = \langle (1, 0), (0), (0) \rangle \diamond \langle (0), (0) \rangle$ and $\langle (1, 1, 0), (0), (0), (0) \rangle = \langle (0), (0) \rangle \diamond \langle (1, 0), (0), (0) \rangle$. Later in Ex. 4.10 and Figure 4 we consider the Catalan table $\langle (2, 0, 0), (1, 1, 0), (0), (0), (0), (1, 0), (0) \rangle = \langle (1, 0), (1, 1, 0), (0), (0), (0) \rangle \diamond \langle (0), (1, 0), (0) \rangle$. Another example will be given in Ex. A.2.

The composition \bullet of Catalan tuples is extended as follows to Catalan tables:

Definition 4.5 (\blacklozenge -operation). The operation $\blacklozenge : \mathcal{T}_k \times \mathcal{T}_l \rightarrow \mathcal{T}_{k+l}$ is given by

$$\langle \tilde{e}^{(0)}, \dots, \tilde{e}^{(k)} \rangle \blacklozenge \langle \tilde{f}^{(0)}, \dots, \tilde{f}^{(l)} \rangle := \langle \tilde{e}^{(0)}, \tilde{e}^{(1)} \bullet \tilde{f}^{(0)}, \tilde{f}^{(1)}, \dots, \tilde{f}^{(l)}, \tilde{e}^{(2)}, \dots, \tilde{e}^{(k)} \rangle .$$

If the 1st pocket has length ≥ 1 , it uniquely factors as $\tilde{e}^{(1)} \bullet \tilde{f}^{(0)}$, and we extract

$$\hat{l} := \sigma_{|\tilde{e}^{(0)}|+|\tilde{e}^{(1)}|+1} \left((1+|\tilde{e}^{(0)}|, |\tilde{e}^{(1)} \bullet \tilde{f}^{(0)}|, |\tilde{f}^{(1)}|, \dots, |\tilde{f}^{(l)}|, |\tilde{e}^{(2)}|, \dots, |\tilde{e}^{(k)}|) \right) . \quad (11)$$

By construction $\hat{l} = l$, and \blacklozenge is uniquely reverted. Note also that Catalan tables $\langle \tilde{e}_0, (0), \tilde{e}_2, \dots, \tilde{e}_k \rangle$ do not have a \blacklozenge -decomposition.

Example 4.6. We have $\langle (0), (2, 0, 0), (0), (0) \rangle = \langle (0), (1, 0), (0) \rangle \blacklozenge \langle (0), (0) \rangle$ and $\langle (0), (1, 1, 0), (0), (0) \rangle = \langle (0), (0) \rangle \blacklozenge \langle (1, 0), (0), (0) \rangle$. Later in Ex. 4.10 and Figure 4 we consider the Catalan table $\langle (2, 0, 0), (1, 1, 0), (0), (0), (0), (1, 0), (0) \rangle = \langle (2, 0, 0), (0), (0), (1, 0), (0) \rangle \blacklozenge \langle (1, 0), (0), (0) \rangle$. Another example will be given in Ex. A.3.

Notice that there is only one condition that determines whether a Catalan table $T = \langle \tilde{e}^{(0)}, \dots, \tilde{e}^{(k)} \rangle$ has a \diamond -reversion and/or a \blacklozenge -reversion. These are $|\tilde{e}^{(0)}| \geq 1$ and $|\tilde{e}^{(1)}| \geq 1$ respectively. The following definition explains how to obtain a term of $G^{(N)}$ out of a Catalan table.

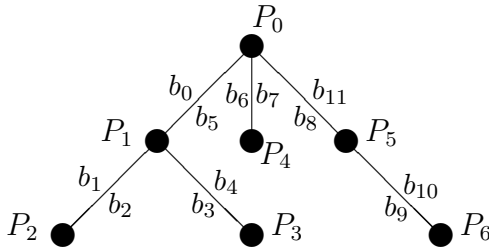
Definition 4.7. To a Catalan table $T_{k+1} = \langle \tilde{e}^{(0)}, \tilde{e}^{(1)}, \dots, \tilde{e}^{(k+1)} \rangle \in \mathcal{T}_{k+1}$ with $N/2 = k + 1$ we associate a monomial $[T]_{b_0, \dots, b_{N-1}}$ in $G_{b_l b_m}$ and $\frac{1}{E_{b_l} - E_{b_m}}$ as follows:

1. Build the pocket tree for the length tuple $(1 + |\tilde{e}^{(0)}|, |\tilde{e}^{(1)}|, \dots, |\tilde{e}^{(k+1)}|) \in \mathcal{C}_{k+1}$. It has $k + 1$ edges and every edge has two sides. Starting from the root and turning counterclockwise, label the edge sides in consecutive order¹ from b_0 to b_{N-1} . An edge labelled $b_l b_m$ encodes a factor $G_{b_l b_m}$ in $G_{b_0, \dots, b_{N-1}}^{(N)}$.
2. Label the $k + 2$ vertices of the pocket tree by P_0, \dots, P_{k+1} in consecutive order¹ when turning counterclockwise around the tree. Let $v(P_m)$ be the valency of vertex P_m (number of edges attached to P_m) and L_m the distance between P_m and the root P_0 (number of edges in shortest path between P_m and P_0).
3. For every vertex P_m that is not a leaf, read off the $2v(P_m)$ side labels of edges connected to P_m . Draw two rows of $v(P_m)$ nodes each. Label the nodes of the first row by the even edge side labels in natural order, i.e. starting at the edge closest to the root and proceed in the counterclockwise direction. Label the nodes of the other row by the odd edge side labels using the same edge order. Take the m -th Catalan tuple $\tilde{e}^{(m)}$ of the Catalan table. If L_m is even, draw the $\left\{ \begin{smallmatrix} \text{direct} \\ \text{opposite} \end{smallmatrix} \right\}$ tree encoded by $\tilde{e}^{(m)}$ between the row of $\left\{ \begin{smallmatrix} \text{even} \\ \text{odd} \end{smallmatrix} \right\}$ nodes. If L_m is odd, draw the $\left\{ \begin{smallmatrix} \text{opposite} \\ \text{direct} \end{smallmatrix} \right\}$ tree encoded by $\tilde{e}^{(m)}$ between the row of $\left\{ \begin{smallmatrix} \text{even} \\ \text{odd} \end{smallmatrix} \right\}$ nodes. Encode a thread from b_l to b_m in the direct or opposite tree by a factor $\frac{1}{E_{b_l} - E_{b_m}}$.

Remark 4.8. In proofs below we sometimes have to insist that one side label of a pocket edge is a particular b_k , whereas the label of the other side does not matter. In such a situation we will label the other side by $b_{\bar{k}}$. Note that if b_k is $\left\{ \begin{smallmatrix} \text{even} \\ \text{odd} \end{smallmatrix} \right\}$ then $b_{\bar{k}}$ is $\left\{ \begin{smallmatrix} \text{odd} \\ \text{even} \end{smallmatrix} \right\}$.

Remark 4.9. For the purpose of this article it is sufficient to mention that an explicit construction for the level function $L_m : \mathcal{C}_{k+1} \rightarrow \{0, \dots, k\}$ exists.

Example 4.10. Later in Fig. 4 we give a diagrammatic representation of the Catalan table $\langle (2, 0, 0), (1, 1, 0), (0), (0), (0), (1, 0), (0) \rangle \in \mathcal{T}_6$. Its length tuple is $(3, 2, 0, 0, 0, 1, 0) \in \mathcal{C}_6$, which defines the pocket tree:



¹This is the same order as in [3, Fig. 5.14].

The edge side labels encode

$$G_{b_0b_5}G_{b_1b_2}G_{b_3b_4}G_{b_6b_7}G_{b_8b_{11}}G_{b_9b_{10}} \cdot$$

For vertex P_0 , at even distance, we draw direct and opposite tree encoded in $\tilde{e}^{(0)} = (2, 0, 0)$:



For vertex P_1 , at odd distance, we draw opposite and direct tree encoded in $\tilde{e}^{(1)} = (1, 1, 0)$:



For vertex P_5 , at odd distance, we draw opposite and rooted tree encoded in $\tilde{e}^{(5)} = (1, 0)$:



They give rise to a factor

$$\frac{1}{(E_{b_0} - E_{b_6})(E_{b_0} - E_{b_8})(E_{b_0} - E_{b_4})(E_{b_2} - E_{b_4})(E_{b_8} - E_{b_{10}})} \times \frac{1}{(E_{b_5} - E_{b_7})(E_{b_5} - E_{b_{11}})(E_{b_5} - E_{b_1})(E_{b_1} - E_{b_3})(E_{b_{11}} - E_{b_9})}.$$

5 The recursion in Catalan tables

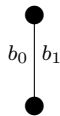
The following theorem shows that the Catalan tables correspond bijectively to the terms in the expansion of the recursion relation (2).

Theorem 5.1. *The recursion (2) of N -point functions in the quartic matrix model (1) has the explicit solution*

$$G_{b_0 \dots b_{N-1}}^{(N)} = \sum_{T \in \mathcal{T}_{k+1}} [T]_{b_0 \dots b_{N-1}},$$

where the sum is over all Catalan tables of length $N/2 = k + 1$ and the monomials $[T]_{b_0 \dots b_{N-1}}$ are described in Definition 4.7.

Proof. We proceed by induction in N . For $N = 2$ the only term in the 2-point function corresponds to the Catalan table $\langle (0), (0) \rangle \in \mathcal{T}_1$. Its associated length tuple $(1, 0)$ encodes the pocket tree



whose single edge corresponds to a factor $G_{b_0 b_1}$. The Catalan tuples of both pockets have length 0, so that there is no denominator.

For any contribution to $G^{(N)}$ with $N \geq 4$, encoded by a length- $N/2$ Catalan table $T_{N/2}$, it must be shown that $T_{N/2}$ splits in one or two ways into smaller Catalan tables whose corresponding monomials produce $T_{N/2}$ via (2). There are three cases to consider.

[I] Let $T_{k+1} = \langle (0), \tilde{e}^{(1)}, \dots, \tilde{e}^{(k+1)} \rangle \in \mathcal{T}_{k+1}$ with $N/2 = k + 1$.

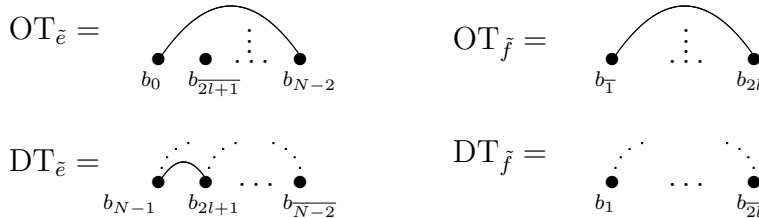
It follows from Definition 4.5 that there are uniquely defined Catalan tables $T_l = \langle \tilde{f}, \tilde{e}^{(2)}, \dots, \tilde{e}^{(l+1)} \rangle \in \mathcal{T}_l$ and $T_{k-l+1} = \langle (0), \tilde{e}, \tilde{e}^{(l+2)}, \dots, \tilde{e}^{(k+1)} \rangle \in \mathcal{T}_{k-l+1}$ with $\tilde{e}^{(1)} = \tilde{e} \bullet \tilde{f}$ and consequently $T_{k-l+1} \blacklozenge T_l = T_{k+1}$. The length $l = \hat{l}$ is obtained via (11). Recall that T_{k+1} cannot be obtained by the \blacklozenge -composition because the zeroth pocket has length $|(0)| = 0$. By induction, T_l encodes a unique contribution $[T_l]_{b_1 \dots b_{2l}}$ to $G_{b_1 \dots b_{2l}}^{(2l)}$, and T_{k-l+1} encodes a unique contribution $[T_{k-l+1}]_{b_0 b_{2l+1} \dots b_{N-1}}$ to $G_{b_0 b_{2l+1} \dots b_{N-1}}^{(N-2l)}$. We have to show that

$$\frac{[T_l]_{b_1 \dots b_{2l}} [T_{k-l+1}]_{b_0 b_{2l+1} \dots b_{N-1}}}{(E_{b_0} - E_{b_{2l}})(E_{b_1} - E_{b_{N-1}})}$$

agrees with $[T_{k+1}]_{b_0 \dots b_{N-1}}$ encoded by T_{k+1} . A detail of the pocket tree of T_{k+1} sketching P_0, P_1 and their attached edges is



Only the gluing of the direct and opposite tree encoded by $\tilde{e} = (e_0, \dots, e_p)$ with the direct and opposite tree encoded by $\tilde{f} = (f_0, \dots, f_q)$ via a thread from b_0 to b_{2l} and a thread from b_{N-1} to b_1 remains to be shown; edge sides encoding $G^{(2)}$ and all other pockets are automatic. A symbolic notation is used now to sketch the trees. Horizontal dots are used to indicate a general direct tree and horizontal dots with vertical dots above them indicate an opposite tree. Unspecified threads are indicated by dotted half-edges. The four trees mentioned above are depicted as

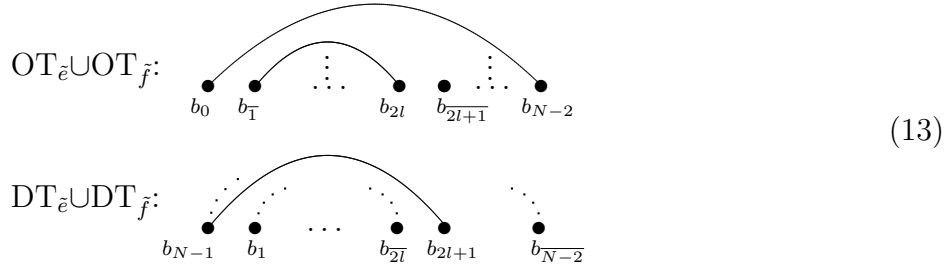


Here \tilde{e} describes P_1 , at odd distance, so that even-labelled nodes are connected by the opposite tree. Every edge in the pocket tree has two sides labelled b_r ,

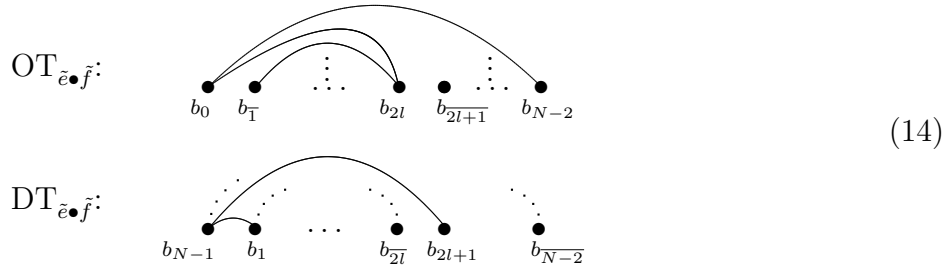
and b_s , where the convention of Remark 4.8 is used when the other side label does not matter.

The first edge in the pocket tree has side labels $b_0 b_{N-1}$ and descends from the root pocket. The following edge is $b_{\overline{2l+1}} b_{2l+1}$ where $2l+2 \leq \overline{2l+1} \leq N-2$ is an even number. The final edge is $b_{N-2} b_{\overline{N-2}}$ where $2l+1 \leq \overline{N-2} \leq N-3$ is an odd number.

Next, \tilde{f} encodes P_0 in the pocket tree belonging to $[T_l]_{b_1 \dots b_{2l}}$. It lies at even distance, but, because the labels at $G_{b_1 \dots b_{2l}}^{(2l)}$ start with an odd one, the odd nodes of \tilde{f} are connected by the direct tree and the even nodes by the opposite tree. Again, $2 \leq \bar{1} \leq 2l$ denotes an even number and $1 \leq \overline{2l} \leq 2l-1$ an odd number. When pasting \tilde{f} into \tilde{e} , the first edge remains $b_0 b_{N-1}$, which descends from the root. Then all edges from \tilde{f} follow and, finally, the remaining edges of \tilde{e} . Thus, before taking the denominators into account, the four trees are arranged as:



The denominator $\frac{1}{(E_{b_0} - E_{b_{2l}})(E_{b_{N-1}} - E_{b_1})}$ (with rearranged sign) corresponds to a thread between the nodes b_0 and b_{2l} and one between the nodes b_{N-1} and b_1 :



The result is precisely described by $\tilde{e} \bullet \tilde{f} = (e_0 + 1, f_0, \dots, f_q, e_1, \dots, e_p)$ with Definitions 3.7 and 3.8. Indeed, the increased zeroth entry corresponds to one additional half-thread attached to the first node b_{N-1} and one additional half-thread to b_0 . For the direct tree the rules imply that the next node, b_1 , is connected to b_{N-1} . This is the new thread from the denominators. The next operations are done within \tilde{f} , labelled $b_1, \dots, b_{\overline{2l}}$, without any change. Arriving at its final node $b_{\overline{2l}}$ all half-threads of \tilde{f} are connected. The next node, labelled b_{2l+1} , connects to the previous open half-thread, which is the very first node b_{N-1} . These and all the following connections arise within \tilde{e}

and remain unchanged. Similarly, in the opposite tree, we first open $e_0 + 1$ half-threads at the zeroth node b_0 . Since $f_0 > 0$, we subsequently open f_0 half-threads at the first node $b_{\bar{1}}$. The next operations remain unchanged, until we arrive at the final node b_{2l} of \tilde{f} . It corresponds to $f_q = 0$, so that we connect it to all previous open half-threads, first within \tilde{f} . However, because $e_0 + 1 > 0$, it is connected by an additional thread to b_0 and encodes the denominator $\frac{1}{E_{b_0} - E_{b_{2l}}}$. This consumes the additional half-thread attached to b_0 . All further connections are the same as within \tilde{e} . In conclusion, we obtain precisely the Catalan table $T_{k+1} = \langle (0), \tilde{e}^{(1)} \dots \tilde{e}^{(N/2)} \rangle$ we started with.

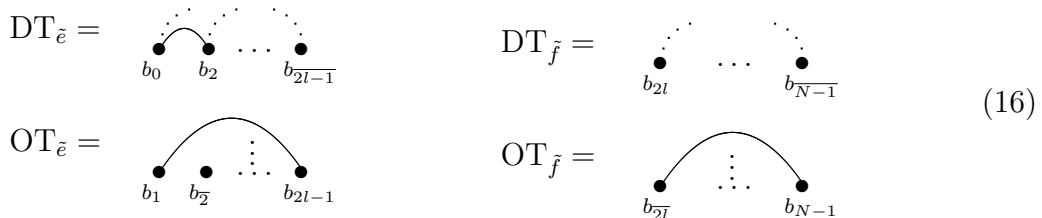
[II] Let $T_{k+1} = \langle \tilde{e}^{(0)}, (0), \tilde{e}^{(2)}, \dots, \tilde{e}^{(k+1)} \rangle \in \mathcal{T}_{k+1}$ and $N/2 = k + 1$. There are uniquely defined Catalan tables $T_l = \langle \tilde{e}, (0), \tilde{e}^{(2)}, \dots, \tilde{e}^{(l)} \rangle \in \mathcal{T}_l$ and $T_{k-l+1} = \langle \tilde{f}, \tilde{e}^{(l+1)}, \dots, \tilde{e}^{(k+1)} \rangle \in \mathcal{T}_{k-l+1}$ with $\tilde{e}^{(0)} = \tilde{e} \circ \tilde{f}$ and, consequently, $T_l \diamond T_{k-l+1} = T_{k+1}$. The length $l = \hat{k}$ is obtained via (10). Recall that T_{k+1} cannot be obtained by the \diamond -composition, because the first entry has length $|(0)| = 0$. By the induction hypothesis, T_l encodes a unique contribution $[T_l]_{b_0 \dots b_{2l-1}}$ to $G_{b_0 \dots b_{2l-1}}^{(2l)}$ and T_{k-l+1} encodes a unique contribution $[T_{k-l+1}]_{b_{2l} \dots b_{N-1}}$ to $G_{b_{2l} \dots b_{N-1}}^{(N-2l)}$. It remains to be shown that

$$\frac{[T_l]_{b_0 \dots b_{2l-1}} [T_{k-l+1}]_{b_{2l} \dots b_{N-1}}}{(E_{b_0} - E_{b_{2l}})(E_{b_1} - E_{b_{N-1}})}$$

agrees with $[T_{k+1}]_{b_0 \dots b_{N-1}}$ encoded by T_{k+1} . A detail of the pocket tree of T_{k+1} sketching P_0, P_1 and their attached edges is

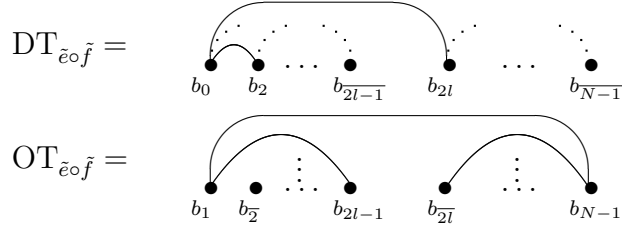


As in case [I] only the gluing of the direct and opposite tree encoded by $\tilde{e} = (e_0, \dots, e_p)$ with the direct and opposite tree encoded by $\tilde{f} = (f_0, \dots, f_q)$ via a thread from b_0 to b_{2l} and a thread from b_1 to b_{N-1} must be demonstrated. Everything else is automatic. These trees are



The notation is the same as in case [I]. The first pocket P_1 , described by the Catalan tuple (0) , is only 1-valent so that the first edge is labelled $b_0 b_1$. The

direct trees in (16) are put next to each other and a thread between b_0 and b_{2l} is drawn for the denominator $\frac{1}{E_{b_0} - E_{b_{2l}}}$. Similarly, the opposite trees in (16) are put next to each other and a thread between b_1 and b_{N-1} is drawn for the denominator $\frac{1}{E_{b_1} - E_{b_{N-1}}}$:



The result are precisely the direct and opposite trees of the composition $\tilde{e} \circ \tilde{f} = (e_0 + 1, e_1, \dots, e_p, f_0, \dots, f_q)$. The increase $e_0 \rightarrow e_0 + 1$ opens an additional half-thread at b_0 and an additional half-thread at b_1 . In the direct tree, this new half-thread is not used by e_1, \dots, e_p . Only when we are moving to f_0 , labelled b_{2l} , we have to connect it with the last open half-thread, i.e. with b_0 . After that the remaining operations are unchanged compared with \tilde{f} . In the opposite tree, the additional half-thread at b_1 is not used in e_1, \dots, e_p . Because f_0 , labelled $b_{\bar{2l}}$, opens enough half-threads, it is not consumed by f_0, \dots, f_{q-1} either. Then, the last node f_q , labelled b_{N-1} , successively connects to all nodes with open half-threads, including b_1 . In conclusion, we obtain precisely the Catalan table $T_{k+1} = \langle \tilde{e}^{(0)}, (0), \tilde{e}^{(2)} \dots \tilde{e}^{(N/2)} \rangle$ we started with.

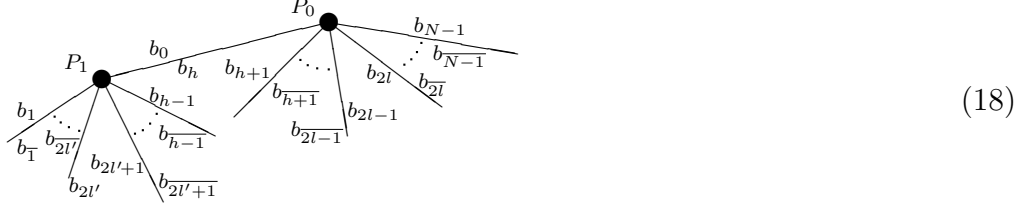
[III] Finally, we consider a general $T_{k+1} = \langle \tilde{e}^{(0)}, \tilde{e}^{(1)}, \tilde{e}^{(2)}, \dots, \tilde{e}^{(k+1)} \rangle \in \mathcal{T}_{k+1}$ with $k+1 = N/2$, $|\tilde{e}^{(0)}| \geq 1$ and $|\tilde{e}^{(1)}| \geq 1$. There are uniquely defined Catalan tables $T_l = \langle \tilde{e}, \tilde{e}^{(1)}, \tilde{e}^{(2)}, \dots, \tilde{e}^{(l)} \rangle \in \mathcal{T}_l$ and $T_{k-l+1} = \langle \tilde{f}, \tilde{e}^{(l+1)}, \dots, \tilde{e}^{(k+1)} \rangle \in \mathcal{T}_{k-l+1}$ with $\tilde{e}^{(0)} = \tilde{e} \circ \tilde{f}$ and consequently $T_l \diamond T_{k-l+1} = T_{k+1}$. Moreover, uniquely defined Catalan tables $T_{l'} = \langle \tilde{f}', \tilde{e}^{(2)}, \dots, \tilde{e}^{(l'+1)} \rangle \in \mathcal{T}_{l'}$ and $T_{k-l'+1} = \langle \tilde{e}^{(0)}, \tilde{e}', \tilde{e}^{(l'+2)}, \dots, \tilde{e}^{(k+1)} \rangle \in \mathcal{T}_{k-l'+1}$ exist, such that $\tilde{e}^{(1)} = \tilde{e}' \bullet \tilde{f}'$ and consequently $T_{k-l'+1} \blacklozenge T_{l'} = T_{k+1}$. We necessarily have $l' \leq k-1$ and $l \geq 2$, because $l' = k$ corresponds to case [I] and $l = 1$ to case [II]. By the induction hypothesis, these Catalan subtables encode unique contributions $[T_l]_{b_0 \dots b_{2l-1}}$ to $G_{b_0 \dots b_{2l-1}}^{(2l)}$, $[T_{k-l+1}]_{b_{2l} \dots b_{N-1}}$ to $G_{b_{2l} \dots b_{N-1}}^{(N-2l)}$, $[T_{l'}]_{b_1 \dots b_{2l'}}$ to $G_{b_1 \dots b_{2l'}}^{(2l')}$ and $[T_{k-l'+1}]_{b_0 b_{2l'+1} \dots b_{N-1}}$ to $G_{b_0 b_{2l'+1} \dots b_{N-1}}^{(N-2l')}$. We have to show that

$$\frac{[T_l]_{b_0 \dots b_{2l-1}} [T_{N/2-l}]_{b_{2l} \dots b_{N-1}}}{(E_{b_0} - E_{b_{2l}})(E_{b_1} - E_{b_{N-1}})} = \frac{[T_{l'}]_{b_1 \dots b_{2l'}} [T_{N/2-l'}]_{b_0 b_{2l'+1} \dots b_{N-1}}}{(E_{b_0} - E_{b_{2l'}})(E_{b_1} - E_{b_{N-1}})} \quad (17)$$

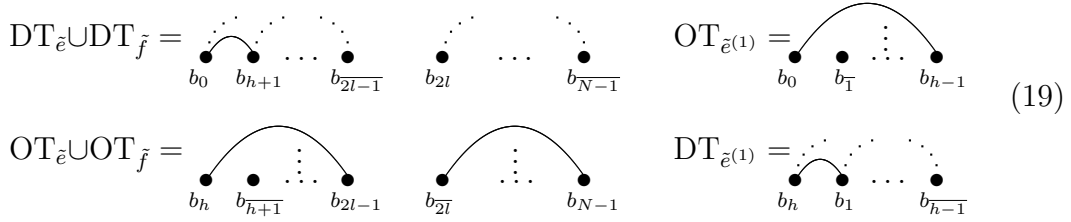
agrees with $[T_{k+1}]_{b_0 \dots b_{N-1}}$.

In the pocket tree of T_{k+1} there must be an edge with side labels $b_0 b_h$, where $3 \leq h \leq N-3$ and h is odd. Here is a detail of the pocket tree of T_{k+1}

showing P_0, P_1 :



The direct and opposite trees for \tilde{e}, \tilde{f} and $\tilde{e}^{(1)}$ can be sketched as



The denominators $\frac{1}{(E_{b_0} - E_{b_{2l}})(E_{b_1} - E_{b_{N-1}})}$ in (17) add threads from b_0 to b_{2l} and from b_1 to b_{N-1} . The first one connects the direct trees for $\tilde{e} \cup \tilde{f}$ to the direct tree encoded by $\tilde{e}^{(0)} = \tilde{e} \circ \tilde{f}$. The second thread does *not* give a valid composition of the opposite trees for $\tilde{e} \cup \tilde{f}$.

This is a problem. The solution is to split this contribution. Half of the contribution is sacrificed to bring the other half in the desired form. Afterwards, the same procedure is repeated for the other term in (17) with a minus-sign. The remainders are the same and cancel each other, whereas the other halves add up to yield the sought monomial.

Returning to trees, we note that in the direct tree for the pocket $\tilde{e}^{(1)}$ there is always a thread from b_h to b_1 , encoding a factor $\frac{1}{E_{b_h} - E_{b_1}}$. With the factor $\frac{1}{E_{b_1} - E_{b_{N-1}}}$ it fulfils

$$\frac{1}{E_{b_h} - E_{b_1}} \cdot \frac{1}{E_{b_1} - E_{b_{N-1}}} = \frac{1}{E_{b_h} - E_{b_1}} \cdot \frac{1}{E_{b_h} - E_{b_{N-1}}} + \frac{1}{E_{b_h} - E_{b_{N-1}}} \cdot \frac{1}{E_{b_1} - E_{b_{N-1}}} \quad (20)$$

The first term on the right-hand side of (20) leaves the direct tree $DT_{\tilde{e}^{(1)}}$ as it is and connects the parts of $OT_{\tilde{e}} \cup OT_{\tilde{f}}$ via the thread from b_h to b_{N-1} to form $OT_{\tilde{e}^{(0)}}$, where $\tilde{e}^{(0)} = \tilde{e} \circ \tilde{f}$.

[*] The final term in (20) also unites $OT_{\tilde{e}} \cup OT_{\tilde{f}}$ and forms $OT_{\tilde{e}^{(0)}}$, but it removes in $DT_{\tilde{e}^{(1)}}$ the thread between b_h and b_1 . It follows from $\tilde{e}^{(1)} = \tilde{e}' \bullet \tilde{f}'$ that this tree falls apart into the subtrees $DT_{\tilde{e}'}$, containing b_h , and $DT_{\tilde{f}'}$, which contains b_1 . These are multiplied by a factor $\frac{1}{E_{b_1} - E_{b_{N-1}}}$. The second term in (17) will remove them.

Indeed, direct and opposite trees for $\tilde{e}^{(0)}$, \tilde{e}' and \tilde{f}' can be sketched as

$$\begin{array}{cc}
\text{DT}_{\tilde{e}^{(0)}} = \begin{array}{c} \cdot \cdot \cdot \cdot \cdot \\ \cdot \quad \cdot \quad \cdot \quad \cdot \quad \cdot \\ b_0 \quad b_{h+1} \quad \dots \quad b_{N-1} \end{array} & \text{OT}_{\tilde{e}'} \cup \text{OT}_{\tilde{f}'} = \begin{array}{c} \cdot \quad \cdot \quad \cdot \quad \cdot \quad \cdot \\ \cdot \quad \cdot \quad \cdot \quad \cdot \quad \cdot \\ b_0 \quad b_{\bar{1}} \quad b_{2l'} \quad b_{2l'+1} \quad b_{h-1} \end{array} \\
\text{OT}_{\tilde{e}^{(0)}} = \begin{array}{c} \cdot \quad \cdot \quad \cdot \quad \cdot \\ \cdot \quad \cdot \quad \cdot \quad \cdot \\ b_h \quad b_{\bar{h+1}} \quad \dots \quad b_{N-1} \end{array} & \text{DT}_{\tilde{e}'} \cup \text{DT}_{\tilde{f}'} = \begin{array}{c} \cdot \quad \cdot \quad \cdot \quad \cdot \quad \cdot \\ \cdot \quad \cdot \quad \cdot \quad \cdot \quad \cdot \\ b_h \quad b_1 \quad b_{2l} \quad b_{2l'+1} \quad b_{h-1} \end{array}
\end{array} \quad (21)$$

The direct tree $\text{DT}_{\tilde{e}^{(0)}}$ remains intact and the thread from b_0 to $b_{2l'}$ encoded in the factor $\frac{1}{(E_{b_0} - E_{b_{2l'}})}$ in (17) connects the opposite trees for $\tilde{e}' \cup \tilde{f}'$ to form the opposite tree for $\tilde{e}^{(1)} = \tilde{e}' \bullet \tilde{f}'$. The direct trees $\text{DT}_{\tilde{e}'} \cup \text{DT}_{\tilde{f}'}$ remain disconnected and are multiplied by $\frac{1}{(E_{b_1} - E_{b_{N-1}})}$ from (17). With the minus-sign from (17) they cancel the terms described in [*]. The other trees combined yield precisely the direct and opposite trees for both $\tilde{e}^{(0)}$ and $\tilde{e}^{(1)}$, so that the single Catalan table we started with is retrieved.

This completes the proof. Bijectivity between Catalan tables and contributing terms to $(N' < N)$ -point functions is essential: Assuming the above construction [I]–[III] missed Catalan subtables $T_l, T_{N/2-l}$, then their composition $T_l \diamond T_{N/2-l}$ would be a new Catalan table of length $N/2$. However, all Catalan tables of length $N/2$ are considered. Similarly for $T_{l'} \blacklozenge T_{N/2-l'}$. \square

This theorem shows that there is a one-to-one correspondence between Catalan tables and the diagrams/terms in $G_{b_0, \dots, b_{N-1}}^{(N)}$ with designated node b_0 . The choice of designated node does not influence $G^{(N)}$, but it does alter its expansion.

Finally, we determine the number d_k of Catalan tables in \mathcal{T}_{k+1} , i.e. the number of different contributions to the $(2k+2)$ -point function $G^{(2k+2)}$. For that we recall:

Proposition 5.2 (Lagrange inversion formula). *Let $\phi(w)$ be analytic at $w = 0$ with $\phi(0) \neq 0$ and $f(w) := \frac{w}{\phi(w)}$. Then the inverse $g(z)$ of $f(w)$, such that $z = f(g(z))$, is analytic at $z = 0$ is given by*

$$g(z) = \sum_{n=1}^{\infty} \frac{z^n}{n!} \frac{d^{n-1}}{dw^{n-1}} \Big|_{w=0} \phi(w)^n .$$

The Lagrange inversion formula is used to prove:

Theorem 5.3. *The number of Catalan tables of length $k+1$ is given by $d_k = \frac{1}{k+1} \binom{3k+1}{k}$ and satisfies*

$$d_k = \sum_{(e_0, \dots, e_{k+1}) \in \mathcal{C}_{k+1}} c_{e_0-1} c_{e_1} \cdots c_{e_k} c_{e_{k+1}} , \quad (22)$$

where $c_k = \frac{1}{k+1} \binom{2k}{k}$ is the k -th Catalan number.

Proof. Let d_{n-1} be the number of Catalan tables of length n . To count d_{k+1} we proceed once more by induction. For $k \geq 1$, the \diamond -product and \blacklozenge -product generate

$$\sum_{l=1}^k 2d_{l-1}d_{k-l}$$

Catalan tables, where some tables are generated twice. These must be subtracted. Only tables with $\tilde{e}^{(1)} = (0)$ or $\tilde{e}^{(0)} = (0)$ are not generated twice. Let there be f_k Catalan tables of length $k+1$ with $\tilde{e}^{(1)} = (0)$. Any of them arises by \diamond -product of smaller Catalan tables, where the left factor must already have $\tilde{e}^{(1)} = (0)$. Therefore, the recursion is

$$f_k = \sum_{l=1}^k f_{l-1}d_{k-l}. \quad (23)$$

The same recursion arises for the number of Catalan tables of length $k+1$ with $\tilde{e}^{(0)} = (0)$ via the \blacklozenge -product. Also the starting points are the same, so there are equally many of both.

We conclude that the total number of Catalan tables satisfies

$$d_k = \left(\sum_{l=1}^k 2d_{l-1}d_{k-l} \right) - \frac{1}{2} \left(-2f_k + \sum_{l=1}^k 2d_{l-1}d_{k-l} \right) = f_k + \sum_{l=1}^k d_{l-1}d_{k-l}. \quad (24)$$

The starting points $f_0 = 1$ and $d_0 = 1$ yield

$$f_k = \frac{1}{2k+1} \binom{3k}{k} \quad \text{and} \quad d_k = \frac{1}{k+1} \binom{3k+1}{k}. \quad (25)$$

To see this, observe that the recursion relations (23) and (24) give rise to generating functions

$$H(x) = \sum_{n=0}^{\infty} f_n x^{n+1} \quad \text{and} \quad G(x) = \sum_{n=0}^{\infty} d_n x^{n+1} \quad (26)$$

satisfying

$$H(x) = H(x) \cdot G(x) + x \quad \text{and} \quad G(x) = G(x) \cdot G(x) + H(x)$$

with $G(0) = 0$ and $H(0) = 0$. Multiplying the first equation by $G(x)$ and the second one by $H(x)$ gives $x \cdot G(x) = H^2(x)$, which disentangles the equations into

$$\frac{1}{x} H^3(x) - H(x) + x = 0, \quad G(x)(1 - G(x))^2 = x, \quad (27)$$

The coefficients (25) can now be obtained by the Lagrange inversion formula. The second equation of (27) results by taking $f(w) = w(1-w)^2$ in Proposition 5.2, i.e. $\phi(w) = \frac{1}{(1-w)^2}$. The coefficients follow then by

$$\begin{aligned} G(x) &= \sum_{n=1}^{\infty} \frac{x^n}{n!} \frac{d^{n-1}}{dw^{n-1}} \Big|_{w=0} \frac{1}{(1-w)^{2n}} \\ &= \sum_{n=1}^{\infty} \frac{x^n}{n!} (2n)(2n+1)\dots(2n+n-2) \\ &= \sum_{n=1}^{\infty} \frac{(3n-2)!}{n!(2n-1)!} x^n = \sum_{n=0}^{\infty} \frac{(3n+1)!}{(n+1)!(2n+1)!} x^{n+1} = \sum_{n=0}^{\infty} d_n x^{n+1}. \end{aligned}$$

For the first equation of (27), set $\frac{H(x)}{\sqrt{x}} = w$, $z = \sqrt{x}$ and $\phi(w) = \frac{1}{1-w^2}$ in Proposition 5.2. Then

$$\begin{aligned} H(x) &= \sqrt{x} \sum_{n=1}^{\infty} \frac{\sqrt{x}^n}{n!} \frac{d^{n-1}}{dw^{n-1}} \Big|_{w=0} \frac{1}{(1-w^2)^n} \\ &= \sum_{n=1}^{\infty} \frac{\sqrt{x}^{n+1}}{n!} \frac{d^{n-1}}{dw^{n-1}} \Big|_{w=0} \sum_{k=0}^{\infty} \binom{n+k-1}{k} w^{2k} \\ &= \sum_{k=0}^{\infty} \frac{x^{k+1}}{(2k+1)!} \binom{3k}{k} \cdot (2k)! . \end{aligned}$$

The other way of generating all Catalan tables is the constructive way. Sum over all pocket trees and multiply the number of Catalan tuples for every pocket must yield the same number. This proves (22). \square

Remark 5.4. The second equation (27) for $G(x)$ is a higher-order variant of the equation $C(x)(1-C(x)) = x$ for the generating function $C(x) = \sum_{n=0}^{\infty} c_n x^{n+1}$ of Catalan numbers.

Remark 5.5. The cubic equation (27) in H which determines the f_k can also be solved by the trigonometric identity

$$\sin^3(\varphi) - \frac{3}{4} \sin(\varphi) + \frac{1}{4} \sin(3\varphi) = 0 ,$$

so that

$$H(x) = \frac{2\sqrt{x}}{\sqrt{3}} \sin\left(\frac{1}{3} \arcsin\left(\frac{3\sqrt{3x}}{2}\right)\right) , \quad G(x) = \frac{4}{3} \sin^2\left(\frac{1}{3} \arcsin\left(\frac{3\sqrt{3x}}{2}\right)\right) .$$

For convenience, the obtained numbers are listed in Table 2. More information about the integer sequences d_k (A006013) and f_k (A001764) can be found via [7] and [8], respectively.

k	N	c_k	c_{k+1}	d_k	f_k
0	2	1	1	1	1
1	4	1	2	2	1
2	6	2	5	7	3
3	8	5	14	30	12
4	10	14	42	143	55
5	12	42	132	728	273
6	14	132	429	3876	1428
7	16	429	1430	21318	7752
8	18	1430	4862	120175	43263

Table 2: The obtained numbers d_k counting the first few correlation functions $G^{(2k+2)}$. The shifted Catalan number c_{k+1} counts the number of pocket trees in $G^{(2k+2)}$, i.e. the number of different chord structures (see Appendix A).

A Chord diagrams with threads

For uncovering the combinatorial structure of (2) it was extremely helpful for us to have a graphical presentation as diagrams of chords and threads. To every term of the expansion (3) of an N -point function we associate a diagram as follows:

Definition A.1 (diagrammatic presentation). Draw N nodes on a circle, label them from b_0 to b_{N-1} . Draw a chord (below in green) between b_r, b_s for every factor $G_{b_r b_s}$ in (3) and a thread (below in orange for t, u even, in blue for t, u odd) between b_t, b_u for every factor $\frac{1}{E_{b_t} - E_{b_u}}$. The convention $t < u$ is chosen so that the diagrams come with a sign.

It was already known in [1] that the chords do not cross each other (using cyclic invariance (5)) and the threads do not cross the chords (using (6)). But the combinatorial structure was not understood in [1] and no algorithm for a canonical set of chord diagrams could be given. The present paper fills this gap.

The $N/2 = k+1$ chords in such a diagram divide the circle into $k+2$ pockets. The pocket which contain the arc segment between the designated nodes b_0 and b_{N-1} is by definition the root pocket P_0 . Moving in the counter-clockwise direction, every time a new pocket is entered it is given the next number as index, as in Definition 4.7. The tree of these $k+2$ pockets, connecting vertices if the pockets border each other, is the pocket tree. A pocket is called even (resp. odd) if its index is even (resp. odd).

Inside every even pocket, the orange threads (between even nodes) form the direct tree, the blue threads (between odd nodes) form the opposite tree. Inside every odd pocket, the orange threads (between even nodes) form the opposite tree, the blue threads (between odd nodes) form the direct tree.

The sign τ of the diagram is given by

$$\tau(T) = (-1)^{\sum_{j=1}^{k+1} e_0^{(j)}}, \quad (28)$$

where $e_0^{(j)}$ is the first entry of the Catalan tuple corresponding to a pocket P_j . Indeed, for every pocket that is not a leaf or the root pocket, the chain of odd nodes starts with the highest index, which implies that every thread emanating from this node contributes a factor (-1) to the monomial (3) compared with the lexicographic order chosen there. In words: count for all pockets other than the root pocket the total number K of threads which go from the smallest node into the pocket. The sign is even (odd) if K is even (odd).

Figure 2 and 3 show Catalan tables and chord diagrams of the 4-point function and 6-point function, respectively.

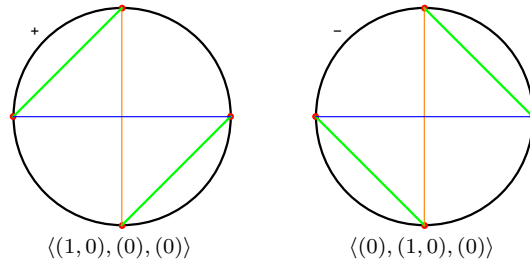


Figure 2: The two chord diagrams and Catalan tables of $G_{b_0 b_1 b_2 b_3}^{(4)}$.

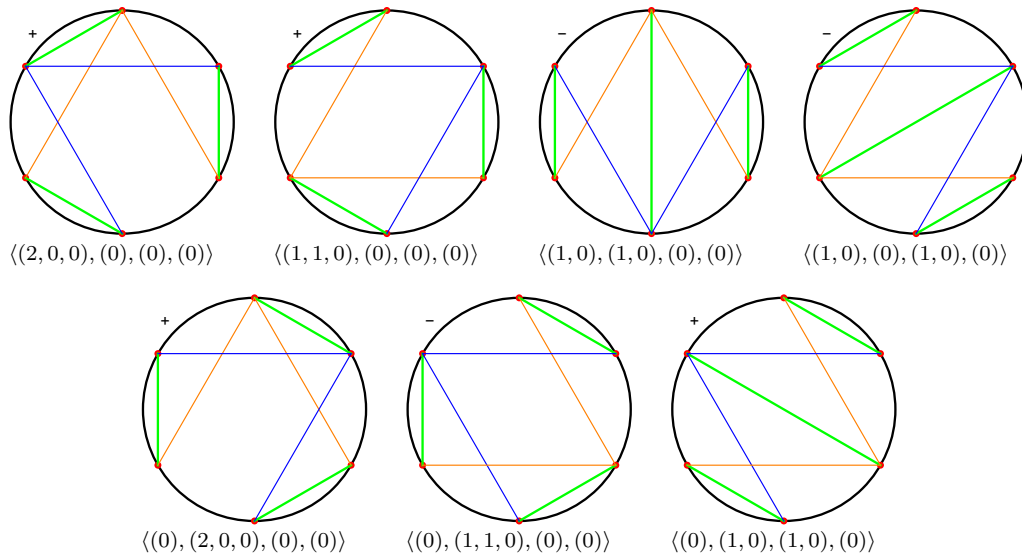
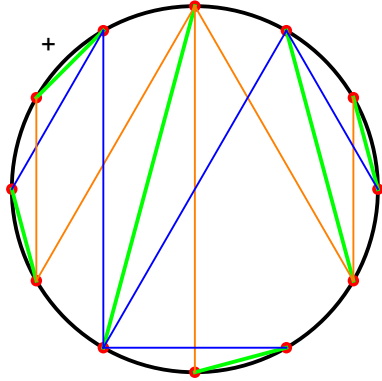


Figure 3: The seven chord diagrams and Catalan tables of $G_{b_0 b_1 b_2 b_3 b_4 b_5}^{(6)}$.

Now that a visual way to study the recursion relation (2) has been introduced, it is much easier to demonstrate the concepts introduced in Secs. 3 and 4.



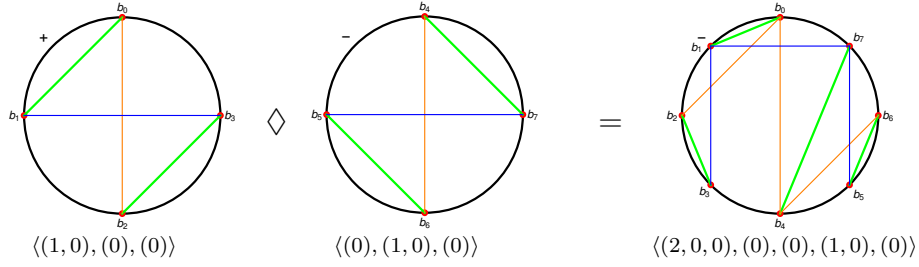
$$\langle (2, 0, 0), (1, 1, 0), (0), (0), (0), (1, 0), (0) \rangle$$

Figure 4: A chord diagram and Catalan table contributing to $G^{(12)}$. Pocket tree and all non-trivial direct and opposite trees have been given in Example 4.10.

Example A.2. The operation \diamond is best demonstrated by an example:

$$\langle (1, 0), (0), (0) \rangle \diamond \langle (0), (1, 0), (0) \rangle = \langle (2, 0, 0), (0), (0), (1, 0), (0) \rangle .$$

The corresponding chord diagrams are



The diagrammatic recipe is to cut both diagrams on the right side of the designated node and paste the second into the first, where the counter-clockwise order of the nodes must be preserved. Then both designated nodes are connected by an orange thread and nodes b_1 and b_{N-1} by a blue thread.

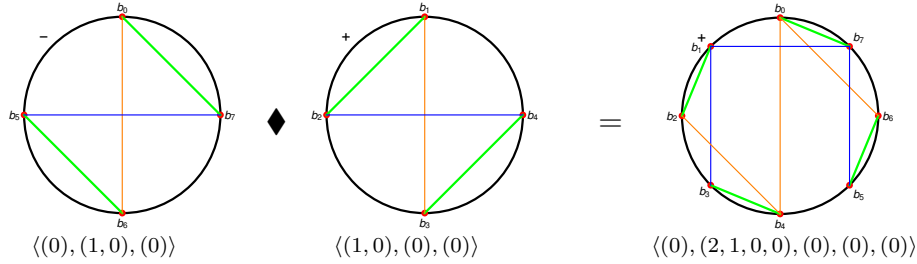
To \diamond -decompose the Catalan table $\langle (2, 0, 0), (0), (0), (1, 0), (0) \rangle$, we first \circ -factorise the zeroth pocket $(2, 0, 0)$ via (8). Here $\sigma_1((2, 0, 0)) = 1$ and, hence, $(2, 0, 0) = (1, 0) \circ (0)$. Next, we evaluate the number \hat{k} defined in (10). We have $1 + |\tilde{f}^{(0)}| = 1$ and $\sigma_1((3, 0, 0, 1, 0)) = 2$. Consequently, we get from Definition 4.3

$$\langle (2, 0, 0), (0), (0), (1, 0), (0) \rangle = \langle (1, 0), (0), (0) \rangle \diamond \langle (0), (1, 0), (0) \rangle .$$

Example A.3. We employ the same example (with diagrams switched) to demonstrate the operation \blacklozenge . In terms of Catalan tables this becomes

$$\langle (0), (1, 0), (0) \rangle \blacklozenge \langle (1, 0), (0), (0) \rangle = \langle (0), (2, 1, 0, 0), (0), (0), (0) \rangle ,$$

for which the chord diagrams are



The diagrammatic recipe is to cut the first diagram on the left side of the designated node and the second diagram on the right side. Then paste the second into the first, where the counter-clockwise order of the nodes must be preserved. The threads in the second diagram switch colours doing so. Then, the designated node of the first diagram is connected to the last node of the second by an orange thread. And the designated node of the second diagram is connected to the last node of the first diagram by a blue thread.

Conversely, to \blacklozenge -decompose the Catalan table $\langle(0), (2, 1, 0, 0), (0), (0), (0)\rangle$, we first \bullet -factorise the first pocket $e^{(1)} = (2, 1, 0, 0)$ via (9). We have $e_0^{(1)} - 1 = 1$, hence consider $\sigma_1((2, 1, 0, 0)) = 2$ and conclude $(2, 1, 0, 0) = (1, 0) \bullet (1, 0)$. Next, we evaluate the number \hat{l} in (11). With $|\tilde{e}^{(0)}| + |\tilde{e}^{(1)}| + 1 = 0 + 1 + 1 = 2$ the decomposition follows from $\sigma_2((1, 3, 0, 0, 0)) = 2$ and yields

$$\langle(0), (2, 1, 0, 0), (0), (0), (0)\rangle = \langle(0), (1, 0), (0)\rangle \blacklozenge \langle(1, 0), (0), (0)\rangle .$$

Acknowledgments

This work was supported by the Deutsche Forschungsgemeinschaft via SFB 878 and the Cluster of Excellence² “Mathematics Münster”.

References

- [1] H. Grosse and R. Wulkenhaar. Self-dual noncommutative ϕ^4 -theory in four dimensions is a non-perturbatively solvable and non-trivial quantum field theory. *Commun. Math. Phys.*, 329:1069–1130, 2014, 1205.0465. doi:10.1007/s00220-014-1906-3.
- [2] R. P. Stanley. Catalan addendum, 2013. URL <http://www-math.mit.edu/~rstan/ec/catadd.pdf>.

²“Gefördert durch die Deutsche Forschungsgemeinschaft (DFG) im Rahmen der Exzellenzstrategie des Bundes und der Länder EXC 2044–390685587, Mathematik Münster: Dynamik–Geometrie–Struktur”

- [3] R. P. Stanley. *Enumerative combinatorics. Vol. 2*, volume 62 of *Cambridge Studies in Advanced Mathematics*. Cambridge University Press, Cambridge, 1999. doi:10.1017/CBO9780511609589.
- [4] B. Eynard and N. Orantin. Mixed correlation functions in the 2-matrix model, and the Bethe ansatz. *JHEP*, 08:028, 2005, hep-th/0504029. doi:10.1088/1126-6708/2005/08/028.
- [5] E. Deutsch and M. Noy. Statistics on non-crossing trees. *Discrete Math.*, 254(1-3):75–87, 2002. doi:10.1016/S0012-365X(01)00366-1.
- [6] M. Noy. Enumeration of noncrossing trees on a circle. In *Proceedings of the 7th Conference on Formal Power Series and Algebraic Combinatorics (Noisy-le-Grand, 1995)*, volume 180, pages 301–313, 1998. doi:10.1016/S0012-365X(97)00121-0.
- [7] A006013. The on-line encyclopedia of integer sequences. URL <https://oeis.org/A006013>.
- [8] A001764. The on-line encyclopedia of integer sequences. URL <https://oeis.org/A001764>.